Lasers Med Sci (2015) 30:875–883
DOI 10.1007/s10103-013-1478-z

ORIGINAL ARTICLE

Gingival tissue healing following Er:YAG laser ablation compared to electrosurgery in rats

Masanori Sawabe · Akira Aoki · Motohiro Komaki · Kengo Iwasaki · Mayumi Ogita · Yuichi Izumi

Received: 1 August 2013 / Accepted: 21 October 2013 / Published online: 16 November 2013

Abstract The erbium-doped yttrium aluminum garnet (Er:YAG) laser is currently used for periodontal soft tissue management with favorable outcomes. However, the process of wound healing after Er:YAG laser (ErL) treatment has not been fully elucidated yet. The aim of this study was to investigate the gingival tissue healing after ErL ablation in comparison with that after electrosurgery (ElS). Gingival defects were created in 28 rats by ablation with ErL irradiation or ElS. The chronological changes in wound healing were evaluated using histological, histometrical, and immunohistochemical analyses. The ErL-ablated gingival tissue revealed much less thermal damage, compared to the ElS. In the ElS sites, the postoperative tissue destruction continued due to thermal damage, while in the ErL sites, tissue degradation was limited and the defects were re-epithelialized early. Heat shock protein (Hsp) 72/73 expression was detected abundantly remote from the wound in the ElS, whereas it was slightly observed in close proximity to the wound in the ErL sites. Hsp47 expression was observed in the entire connective tissue early in the wound healing and was found limited in the wound area later. This phenomenon proceeded faster in the ErL sites than in the ElS sites. Expression of proliferating cell nuclear antigen (PCNA) persisted in the epithelial tissue for a longer period in the ElS than that in the ErL. The ErL results in faster and more favorable gingival wound healing compared to the ElS, suggesting that the ErL is a safe and suitable tool for periodontal soft tissue management.

Keywords Er:YAG laser · Electrosurgery · Wound healing · Histology · Heat shock protein · Proliferating cell nuclear antigen

Introduction

Lasers have been applied for periodontal tissue management such as soft tissue surgery, periodontal pocket treatment, and osseous surgery [1–5]. Unlike conventional periodontal treatment, laser treatment has outstanding features such as easy tissue ablation, strong bactericidal effect, and potential biostimulation in the treated sites [1–6]. Currently, the erbium-doped yttrium aluminum garnet (Er:YAG) laser (ErL) is considered one of the most promising lasers in periodontal therapy because of its favorable clinical performance with less thermal damage in periodontal soft and hard tissue treatment [1, 2, 4, 7–11]. Moreover, ErL delivered with a fine contact tip enables precise and delicate irradiation, which is clinically useful for rigorous soft tissue management, such as gingivectomy, frenectomy, removal of melanin pigmentation and metal tattoos, and crown lengthening, with minimal bleeding [2, 11–15].

Conventionally, electrosurgery (ElS) is also frequently used for soft tissue management in periodontal surgery [16–18]; however, it is well known that the ElS occasionally causes severe thermal damage, delayed wound healing, and postoperative pain to the surrounding tissues [19–22]. In spite of the widespread usage of ErL and ElS, the periodontal soft tissue healing following both treatments has not been assessed in detail.

Heat shock proteins (Hsps) are a highly conserved family of proteins, which play a role in the recovery of cells from

Electronic supplementary material The online version of this article (doi:10.1007/s10103-013-1478-z) contains supplementary material, which is available to authorized users.

M. Sawabe · A. Aoki (✉) · M. Ogita · Y. Izumi
Department of Periodontology, Graduate School of Medical and Dental Sciences, Tokyo Medical and Dental University (TMDU), 1-5-45 Yushima, Bunkyo-ku, Tokyo 113-8549, Japan
e-mail: aoperi@tmd.ac.jp

M. Komaki (✉) · K. Iwasaki
Department of Nanomedicine (DNP), Graduate School of Medical and Dental Sciences, Tokyo Medical and Dental University (TMDU), 1-5-45 Yushima, Bunkyo-ku, Tokyo 113-8549, Japan
e-mail: komaki.peri@tmd.ac.jp

stresses and injuries as intracellular chaperons to maintain synthesis and proper conformation of proteins and to repair damaged proteins [23, 24]. Heat shock protein 70 (Hsp72) has a cytoprotective function, and its expression is induced by cellular stress, including elevated temperature. Hsp72/73 protein chaperones are involved in the refolding of denatured peptides to prevent proteolytic degradation, which is the heat shock response as a part of an eukaryotically conserved phenomenon. Hsp47 is a collagen-binding glycoprotein that supports molecular maturation of collagens [25, 26]. The Hsp47 expression increases in accordance with the increased synthesis of type I collagen and proliferation of cells [27, 28].

In this study, we examined the gingival tissue healing after ErL gingival ablation in comparison with that after ElS. The expression of Hsp72/73, Hsp47, and proliferating cell nuclear antigen (PCNA) was immunohistochemically analyzed for the assessment of thermal influence as well as functional activity and proliferation of cells during wound healing.

Materials and methods

Animals

A total of 28, 9-week-old, male Sprague–Dawley (SD) rats were used. All animals were kept under normal laboratory conditions and fed with standard rat chow and water ad libitum. The protocol of this animal experiment was approved by the Ethical Committee of Animal Research Center of Tokyo Medical and Dental University (no. 0120051A).

Laser and electrosurgical devices

An ErL apparatus (DElight; HOYA Photonics, Fremont, CA), which emits irradiation at a wavelength of 2.94 μm, with an energy output of 30–350 mJ/pulse, a maximum pulse repetition rate of 30 Hz, and a pulse duration of 200 μs, was employed. Energy output was monitored using a power meter (Field Master and detector LM-P10i; Coherent Company, USA). An electrosurgical device (Operer DS-M, J. Morita Mfg. Corp. Kyoto, Japan) with a frequency of 1.2 MHz and a maximal power of 40 W was used.

Experimental procedures

The operation was performed under general anesthesia with 2 % isoflurane (Forene, Abbot Scandinavia Co., Solna, Sweden) in room air using an anesthesia unit (Univentor 400®, Univentor, Zejtun, Malta), with a small mask covering the nose.

Periodontal soft tissue defects were prepared on the gingiva of the maxillary first molars by ErL or ElS device. ErL irradiation was performed at an energy density of 10.4 J/cm^2/pulse and 30 Hz using an 80° curved contact tip made of quartz glass with a diameter of 400 μm and approximately 65 % laser transmission (Fig. S1(A), upper). The energy density and pulse rate were within the usual settings in clinical practice. As for the ElS, an intensity setting of 4.5 (range, 0 to 9) in the cutting mode with a thin contact probe (25 μm in diameter) was used, which is clinically suitable for soft tissue incision (Fig. S1(A), lower). The operating time was approximately 20–30 s without a significant difference in both treatments.

The area from the mesiobuccal angle to the mesiopalatal surface groove was treated. Vertically, gingival ablation was performed until the tip end directly contacted the alveolar bone surface, and the bottom of tissue defect was defined right over the alveolar crest. In the mesial site of gingiva, the approximate defect dimensions were buccolingually 2.0 mm in length, mesiodistally 1.5 mm in width, and vertically 1.0 mm in depth. The contact tip or probe of each device was contacted parallel or slightly oblique to the root axis during root surface debridement. This gingival defect model was created to simulate periodontal soft tissue procedures such as gingivectomy as well as gingival curettage.

Histological analysis

Animals were sacrificed under anesthesia before treatment (nontreated control), immediately after (0 h), 6 h and 1, 3, 6, and 10 days after irradiation (four rats at each time point), and then, the maxillae were resected and fixed in 4 % paraformaldehyde in 0.1 M phosphate buffer (pH 7.4) at 4 °C for 72 h. After decalcification in a 10 % EDTA solution for approximately 4 weeks at 4 °C, the specimens were embedded in paraffin. Sagittal sections through the buccolingual midpoint of the mesial root of maxillary first molar were prepared at 4 μm thickness and stained with hematoxylin–eosin (H-E) or azan. The histological sections were observed under a light microscope (BZ-8000, Keyence, Osaka, Japan). One representative section in the buccolingual midpoint of the root was selected for each group and was compared. The images were captured and measured using an image system software (BZ Analyzer Software, Keyence). In the specimens immediately after surgery (0 h), dimensions of the defects prepared by ErL and ElS were measured. The width of the top and the bottom, the depth, and the area of the defect were determined (Fig. S1(B)).

Immunohistochemical analysis

Deparaffinized and rehydrated sections were incubated for 20 min in 0.3 % hydrogen peroxide in phosphate-buffered saline to inactivate endogenous peroxidase. Nonspecific protein binding was blocked by incubation for 1 h with 0.5 % normal goat serum. Then, individual sections were incubated with one of the following antibodies: mouse anti-Hsp72/73 monoclonal antibody (diluted 1:100; Calbiochem, Darmstadt,

Germany), mouse anti-rat Hsp47 (diluted 1:250; StressGen, Ann Arbor, MI) for 1 h at room temperature and PCNA (diluted 1:100, sc-56; Santa Cruz Biotechnology, Santa Cruz, CA) over night at 4 °C. The sections were then incubated with the appropriate secondary antibodies, Histofine Simple Stain Rat MAX PO (M) (Nichirei Co, Tokyo, Japan) for Hsp72/73 and Hsp47 for 30 min and biotinylated anti-mouse IgG (H + L) affinity purified (Vector Laboratories, inc., Burlingame, CA) for PCNA for 1 h using avidin-biotinylated peroxidase complex method with Vectastain Elite ABC Kit (Vector Laboratories, Inc., Burlingame, CA). Finally, color development was performed with a diaminobenzidine solution (Sigma, St. Louis, MO) and counterstained with eosin. The stained sections were observed under a light microscope.

Histometrical analysis

Based on the extent of red- and pink-colored area surrounding the defect in the azan staining, the thickness of the changed layer (thermal coagulation) in the connective tissue was measured at randomly selected ten different points with equal intervals on the treated surface in one representative section for each rat at 0 h. The ten data points were averaged, and the average was denominated as the representative value of each treatment for each rat ($n=4$). The thickness of the affected layer showing the lack of expression of Hsp72/73 or Hsp47 at 6 h was determined in the same manner. For evaluation of the re-epithelialization of defects, the distance from the nearest end point of epithelial tissue to cement–enamel junction (CEJ) was measured in one representative section for each treatment in each rat at each time point ($n=4$).

Statistical analysis

The changes in parameters of the defect dimensions and widths of the changed or affected layer on the treated connective tissues in the ErL and ElS sites were compared by unpaired Student's t test. The differences in the distance from the end of epithelial tissue to CEJ in both sites were subjected to two-way factorial ANOVA followed by multiple comparisons among the observation period using Dunnett's post hoc test, and the difference in the ErL and ElS sites was subjected to unpaired Student's t test. $p<0.05$ was considered to be statistically significant.

Results

Gross pathology

The ErL ablated gingival tissue effectively without major thermal alteration. Immediately after surgery (0 h), in the ErL sites, marginal gingival tissue showed slight carbonization and coagulation, and bleeding from the gingival defect was frequently observed (Fig. 1(b)). In the ElS sites, marginal gingival tissue showed moderate coagulation with no bleeding (Fig. 1(h)). At

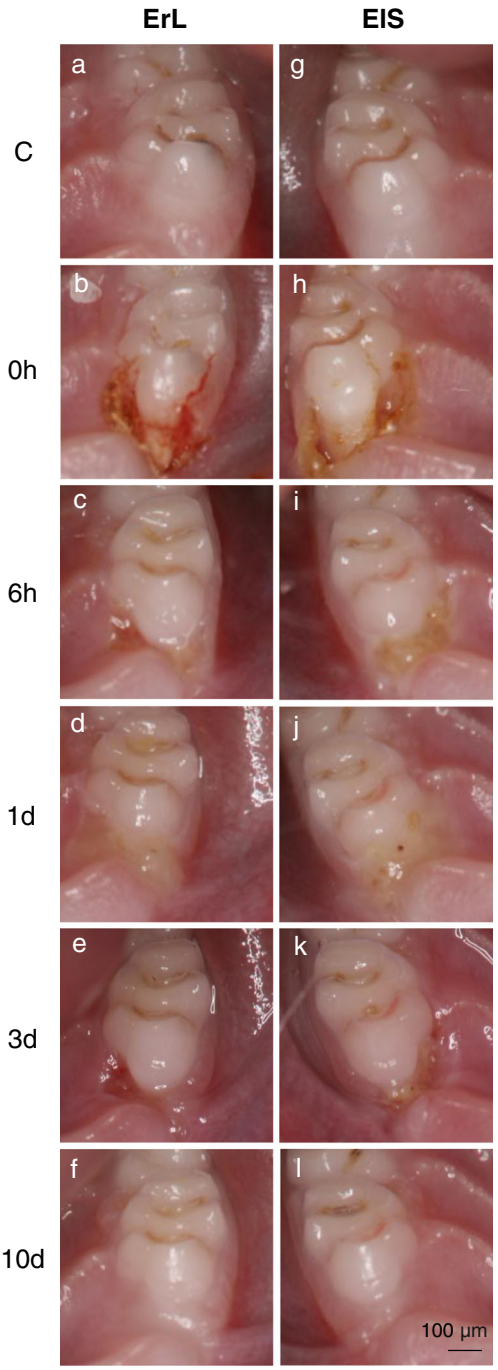

Fig. 1 Gross pathology of gingival tissues showing wound healing following Er:YAG laser (*ErL*) irradiation (*a–f*) or electrosurgery (*ElS*) (*g–l*). Immediately after surgery (0 h), marginal gingiva showed slight carbonization and coagulation with bleeding in the ErL (*b*), whereas moderate coagulation with no bleeding was observed in the ElS (*h*). At 6 h and day 1, pseudomembrane was observed in both sites (*c*, *d*, *i*, *j*). At day 3, in the ErL, re-epithelialization and faster progress of healing were observed (*e*). In the ElS, ulcer formation with pseudomembrane was observed at day 3 (*k*), and re-epithelialization was almost completed at day 6 (data not shown). At day 10, similar wound healing was observed in both sites (*f*, *l*)

6 h and day 1, pseudomembrane was observed on the treated surface in both sites (Fig. 1(c, d, i, j)). In the ErL sites, re-epithelialization was observed at day 3, and wound healing progressed uneventfully (Fig. 1(e)); in contrast, in the ElS sites, ulcer formation with pseudomembrane was still observed at day 3 (Fig. 1(k)), and the re-epithelialization was delayed by day 6 (data not shown). At day 10, both ErL and ElS treatments showed similar wound healing without inflammation (Fig. 1(f, l)).

Histological analysis

In the ErL sites and ElS sites at 0 h, the widths of the top and bottom, the depth, and area of the defect were not significantly different, and gingival defects with almost the same dimensions were prepared in both treatments (Fig. S1(C)).

At 0 h, less thermal coagulation was observed in the ErL sites compared to the ElS sites (Fig. 2(b, i), arrowheads). At 6 h, inflammatory cells had infiltrated around the treated area in both sites (Fig. 2(c, j)). At day 1, faster and more mature fibrin clot formation was observed in the ErL sites than in the ElS sites (Fig. 2(d, k)). From 6 h to day 1, in the ElS, due to thermal damage, the epithelial layer and connective tissue collapsed, and debris consisting of disintegrated necrotized tissue was observed on the top of the defect, which was covered by pseudomembrane (Fig. 2(j, k)). Also, only in the ElS sites, the separation between epithelial layer and connective tissue was observed at 6 h and day 1 (Fig. 2(j, k), arrowheads). By day 3, granulation tissue formation and re-epithelialization of the defect were nearly completed in the ErL sites (Fig. 2(e)), while the re-epithelialization commenced at day 3 and was completed by day 6 in the ElS sites (Fig. 2(l, m)). At day 10, in both sites, the wound repair was completed, except for the immature formation of rete pegs in the epithelial layer as well as incomplete connective tissue maturation in the ElS site.

Immunohistochemical analysis

Hsp72/73 expression

At 0 h, Hsp72/73 was not observed (data not shown) in any of experimental tissue. At 6 h and day 1, in the ErL sites, Hsp72/73 was very slightly or slightly detected in the fibroblasts and blood vessels in gingival connective tissue and periodontal ligament and was not detected or very slightly detected in the dental pulp (Fig. 3(a–c)) as a line concentrically adjacent to

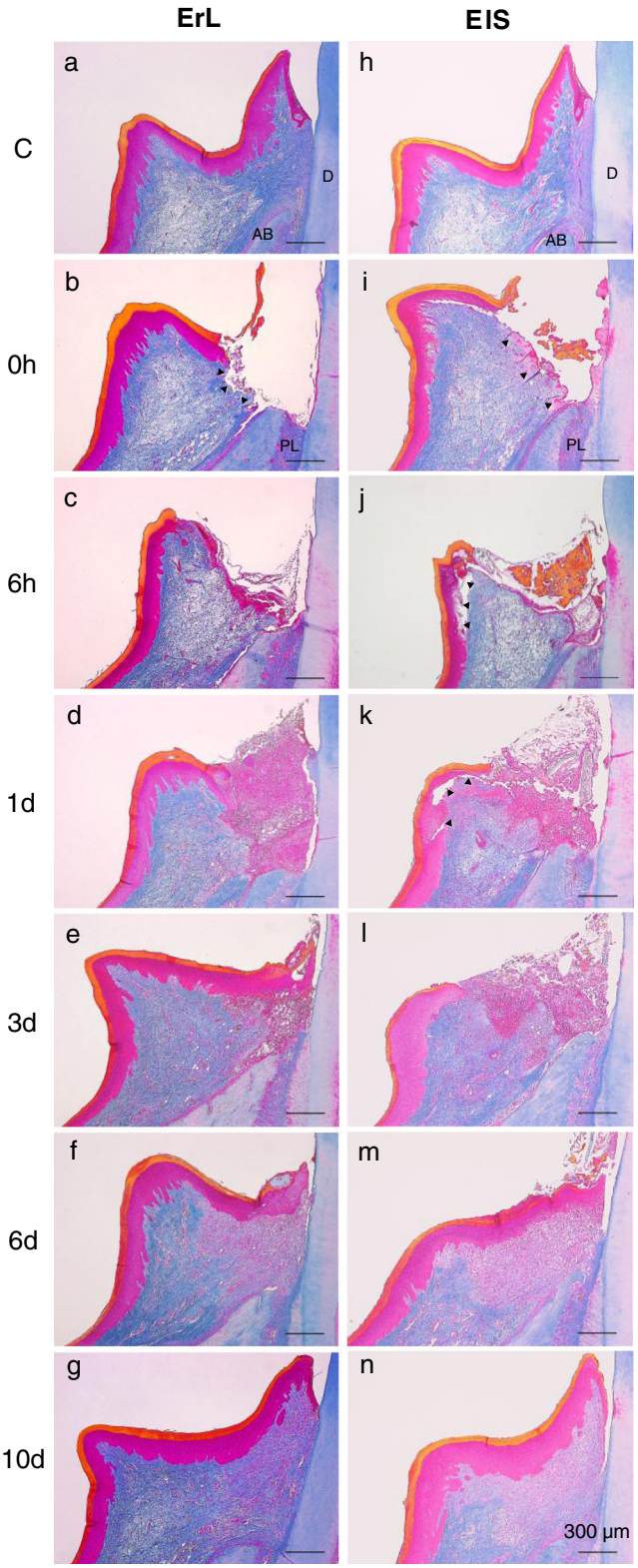

Fig. 2 Histological photomicrographs of the gingival defect following ErL irradiation (*a–g*) or ElS (*h–n*). Before treatment (nontreated control (*C*)), there was no inflammation in the gingiva (*a*, *h*). At 0 h, much less changed (coagulated) layer was observed on the treated connective tissue surface of the gingival defect in the ErL (*b*) than in the ElS (*i*) (*arrowheads*). At day 1, faster and more mature fibrin clot formation was observed in the ErL (*d*) than in the ElS (*k*). In the ErL, re-epithelialization was almost complete at day 3 (*e*), while in the ElS, collapse of the epithelial *(arrowheads)* and connective tissue layer progressed up to day 3 (*j*, *k*, *l*), and re-epithelialization was delayed and completed by day 6 (*m*). Inflammation of gingiva was scarce at both sites at day 10 (*g*, *n*), but connective tissue maturation was delayed in the ElS (*n*). *AB* alveolar bone, *D* root dentin, *PL* periodontal ligament. (Azan stain)

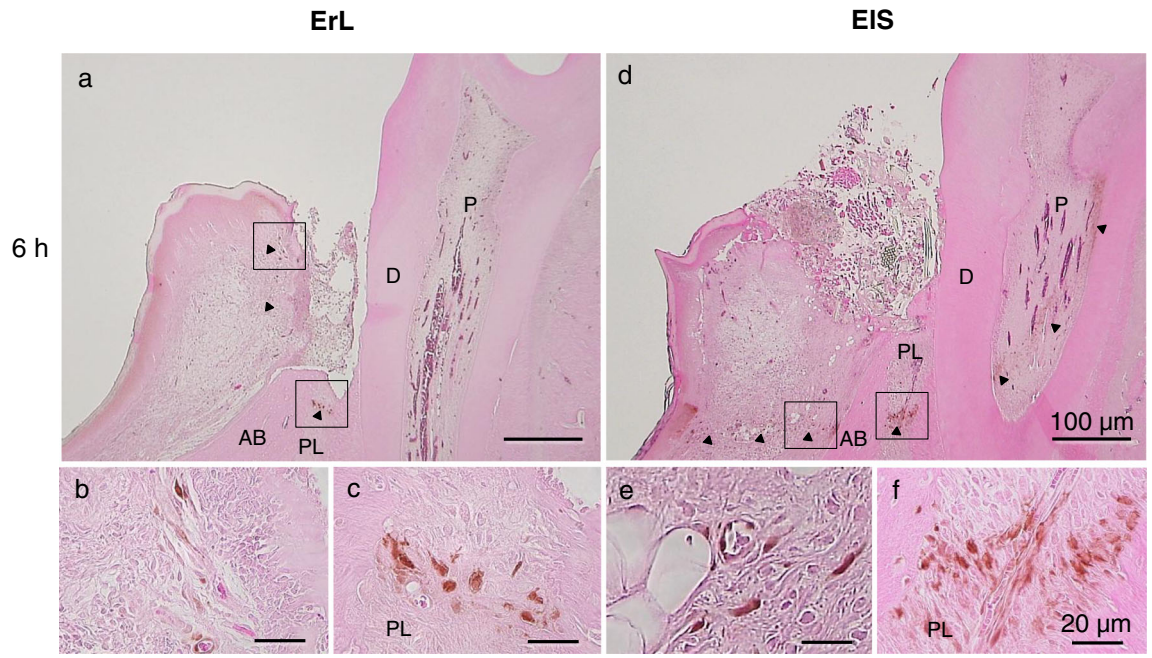

Fig. 3 Immunohistological photomicrographs showing Hsp72/73 expression in the gingival connective tissue, periodontal ligament, and dental pulp of Er:YAG laser (*ErL*) sites (*a*–*c*) and electrosurgery (*ElS*) sites (*d*–*f*). At 6 h, in the ErL sites, Hsp72/73 expression (*arrowheads*) was very slightly or slightly detected in the gingival connective tissue (*a*, *b*) and periodontal ligament (*a*, *c*) and very slightly detected or not detected in the dental pulp (a) adjacent to the ablation defect, while in the ElS sites, intense staining was more abundantly observed in a band-like zone in these tissue remote from the treated site concentrically (*d*, *e*, *f*). *b*, *c*, *e*, *f* Higher magnification of Hsp72/73 expression in fibroblasts and blood vessels in the *square boxes* (a, d) is shown. *AB* alveolar bone, *D* root dentin, *P* dental pulp, *PL* periodontal ligament. (Eosin counterstain)

the ablation defect, while in the ElS sites, intense staining was abundantly observed in a band-like zone in gingival connective tissue, periodontal ligament, and dental pulp (Fig. 3(d–f)) remote from the treated site, concentrically. At day 3, in both sites, Hsp72/73 expression was very slight, and it was no longer detected at day 6 (data not shown).

Hsp47 expression

In the control, constitutive expression of Hsp47 was detected in the fibroblasts and blood vessels, strongly in the connective tissue adhered to the root surface, periodontal ligament, periosteum and sparsely in subepithelial connective tissue and epithelial tissue (basal cells) (Fig. 4(a)). At 0 h, Hsp47 expression was reduced in the connective tissue and periodontal ligament in both treatments (Fig. 4(b, g)). At 6 h, the expression was recovered in the connective and epithelial tissues and periodontal ligament (data not shown). By day 1, the expression in the connective and epithelial tissue was detected adjacent to the defect in the ErL sites (Fig. 4(c), arrowheads) and remote from the defect in the ElS sites (Fig. 4(h), arrowheads), which was later extended to the wound area in accordance with the progression of wound healing. At day 3, in the ErL, Hsp47 expression was detected more broadly and intensely in the whole connective tissue (Fig. 4(d)), whereas the expression was limited to the connective tissue remote from the defect in the ElS (Fig. 4(i)). At days 6 and 10, in the ErL sites, the intense expression area was reduced and limited to the wound area (Fig. 4(e, f)), while in the ElS sites, the expression spread and remained in the entire connective tissue including the wound area (Fig. 4(j, k)).

PCNA expression

After treatment, PCNA expression tended to show an analogous expression as Hsp47 in the connective and epithelial tissues. Regarding the epithelial tissue, PCNA expression was subtle before treatment. At day 1, in both sites, PCNA expression was strongly observed in the epithelial tissue including the basal layer (Fig. S2a, c). At day 6, in the ErL sites, PCNA was scarcely detected (Fig. S2b), whereas the expression still remained in the basal layer in the ElS sites (Fig. S2d), and in the connective tissue under the epithelium, increased PCNA expression was observed in both treatments. At day 10, in the ElS sites, it decreased to a level equal to that of the nontreated control.

Histometrical analysis

Thickness of the thermally changed or affected layer in the gingival connective tissue

The thickness of the changed layer (thermal coagulation) indicated by a pink- and red-colored area in the gingival connective tissue surrounding the defect was significantly

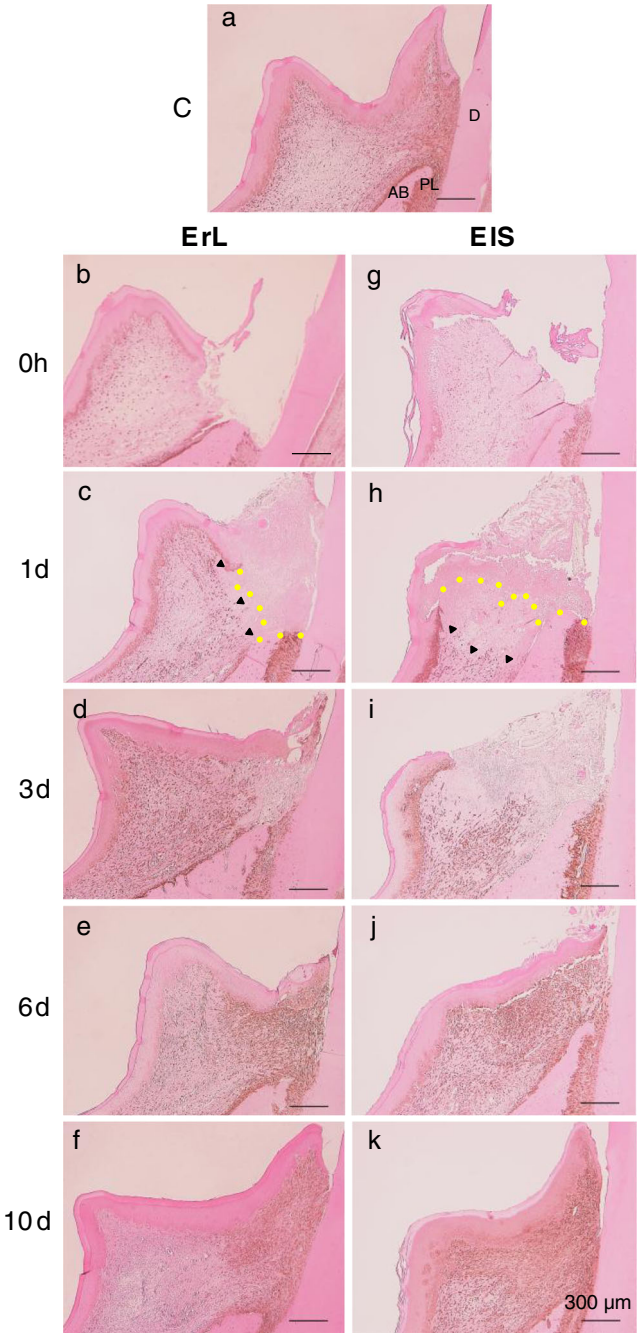

Fig. 4 Immunohistological photomicrographs showing Hsp47 expression in the gingival epithelial and connective tissues and periodontal ligament of the Er:YAG laser (*ErL*) sites (*b–f*) and in the electrosurgery (*ElS*) sites (*g–k*). Immediately after surgery (0 h), Hsp47 expression was reduced than before treatment (nontreated control (*C*)) (*a*). Initially at 6 h, Hsp47 expression was clearly recovered in the periodontal ligament close to the defect in both sites (data not shown). At 6 h and day 1, Hsp47 expression was detected in the intact connective and epithelial tissue close to the ablation defect in the ErL sites (*c*) and remote from the defect area in the ElS sites (*h*) (*arrowheads*) (*dotted line* indicates the border of connective tissue), and later, it gradually moved to the wound healing area. At day 3, in the ErL sites (*d*), Hsp47 was expressed more intensely in the entire connective tissue area than in the ElS sites (*i*). At day 6, in the ErL, Hsp47-expressed area narrowed and moved into the wound area (*e*), and in the ElS, the expression extended into the entire connective tissue (*j*). At day 10, in the ErL, Hsp47 expression was limited to the wound area (*f*), whereas in the ElS, Hsp47 was still observed in the entire connective tissue (*k*). *AB* alveolar bone, *D* root dentin, *PL* periodontal ligament. (Eosin counterstain)

smaller in the ErL sites (21.5±4.6 μm, $n=4$) (Fig. 2(b)) than that in the ElS sites (84.9±15.7 μm, $n=4$) ($p<0.01$) (Fig. 2(i)). The thickness of the affected layer showing the lack of Hsp72/73 expression at 6 h was significantly smaller in the ErL sites (94.0±19.5 μm, $n=4$) than that in the ElS sites (505.0±106.4 μm, $n=4$) ($p<0.05$) (Fig. 3(a, d)). The thickness of the affected layer in the connective tissue showing the lack of immunoreactivity to Hsp47 at 6 h was significantly smaller in the ErL sites (131.4±24.3 μm, $n=4$) than that in the ElS sites (540.7±99.0 μm, $n=4$) ($p<0.01$).

Re-epithelialization process

Immediately after surgery, both treatments exhibited an equal extent of epithelial defects. At 6 h, the distance from the nearest end of epithelial tissue to CEJ became significantly greater than that immediately after surgery in both sites ($p<0.05$), and the ElS sites showed a larger distance than the ErL sites (Fig. 5). By day 1, in the ErL sites, onset of re-epithelialization with normal appearance of epithelium was noted adjacent to the defect, and re-epithelialization proceeded uneventfully; however, in the ElS sites, due to the consecutive degradation of gingival tissue after the procedure, the distance further increased by day 1 ($p<0.01$), resulting in a significantly greater difference between both sites ($p<0.05$) (Figs. 2(d, k) and 5). At day 3, in the ElS sites, commence of re-epithelialization was observed and the distance became smaller and continued decreasing, but the re-epithelialization was markedly delayed (Figs. 2(e, l) and 5). At day 10, both sites showed minimal distance. During the observation period, the distance in the ErL sites was significantly smaller than that in the ElS sites ($p<0.05$) (Fig. 5).

Discussion

Previous clinical and experimental studies have demonstrated that ElS occasionally causes postoperative pain, delayed wound healing, and gingival recession [20–22]. The present study histologically and immunohistochemically demonstrated the following advantageous properties of the ErL compared to the ElS in periodontal soft tissue surgery.

First, the ErL exhibited much less thermal damage than the ElS. Histologically, the thermally changed layer (coagulation) in connective tissue was 20 μm thick immediately after ErL ablation, which was approximately one fourth of the ElS (approximately 85 μm thickness). This finding is comparable to a previous report that the thickness of the changed layer in connective tissue was 10–50 μm after pig skin incision by ErL

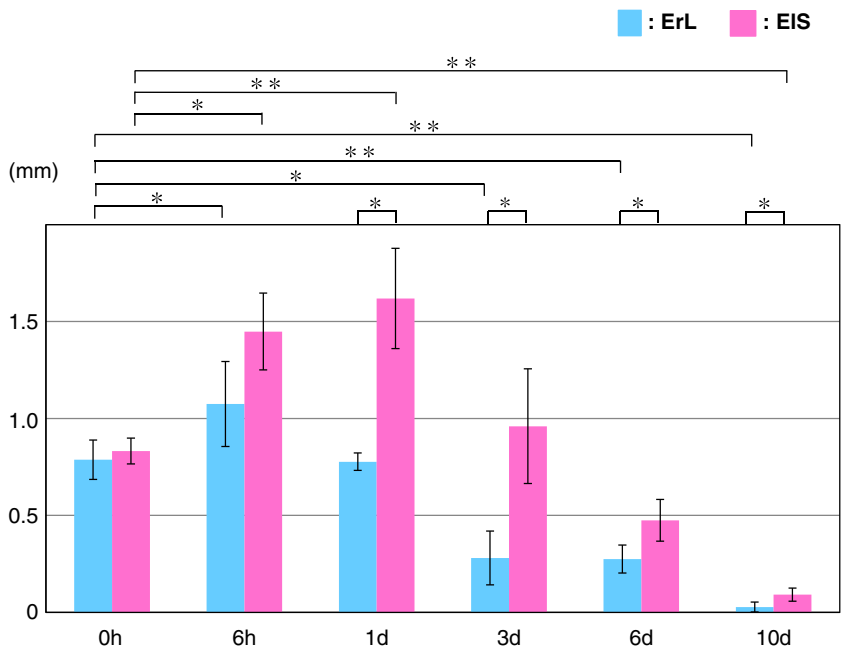

Fig. 5 Histometrical analysis of the distance from cement-enamel junction to the nearest end of epithelial tissue following Er:YAG laser (*ErL*) irradiation and electrosurgery (*ElS*). The distance was not significantly different immediately after surgery (0 h) in both sites, but in the ElS sites, it gradually became longer till day 1. The distance in the ErL sites was significantly shorter than that in the ElS sites from days 1 to 10. $*p<0.05$; $**p<0.01$, a statistically significant difference (a two-way factorial ANOVA followed by Dunnett's post hoc test and unpaired Student's *t* test)

[8]. Secondly, the ErL treatment did not impede wound healing in the early stage, whereas the ElS did due to potentially residual thermal damage. In the ElS sites, the breakdown of the surrounding tissues continued postoperatively, and epithelial and connective tissues gradually degenerated, and ulcer formation persisted till day 3. In fact, in the ElS, the distance between the CEJ and the end of the epithelial tissue became significantly longer over time after surgery and reached maximal at day 1, and the onset of re-epithelialization was delayed. Thus, less thermal damage as well as more bleeding due to the weak thermal effect of the ErL produced more effective fibrin clot and granulation formation in the ErL sites than in the ElS sites, resulting in faster and more favorable wound healing.

Moreover, immunohistochemical analysis using Hsp expression may explain the difference in the degree of invisible thermal influence between the ErL and ElS. Heat shock protein 72/73 (Hsp70) is the first and the most prominent protein found in stressed cells, which plays a significant role in rescuing stressed cells by helping damaged proteins refold or by participating in the synthesis of new proteins [29]. In the present study, Hsp72/73 expression was minimal in gingival connective tissue, periodontal ligament, and dental pulp adjacent to the ablated area in the ErL, whereas in the ElS, it was more clearly detected in a zone remote from the ablation defect. Hsp72/73 expression was reported to occur at a site with a temperature increase of approximately 5 °C [24, 30, 31], which means that the ElS produced an excessive thermal damage in the larger area of surrounding tissues than the ErL. Hsp47, which serves as a reliable functional marker for the activity of connective tissue cells due to its function as a collagen-specific molecular chaperone and its expression under unstressed conditions [27, 32], was also expressed in the connective tissues adjacent to the defect in the ErL and remote from the defect in the ElS after surgery.

Thus, the lack of immunoreactivity to antibody against Hsp72/73 and Hsp47 clearly indicated the presence and area of potential thermal damage in the tissues which was invisible as cellular alterations in the usual histological analysis and was wider than that of the histologically visible changed layer (thermal coagulation). This finding is consistent with the report by Yamasaki et al. [33], which demonstrated that Hsp72/73 expression was detected after CO_2 laser treatment as a band-like zone surrounding the Hsp47-free area adjacent to the defect. Consequently, the visible and invisible thermal alteration of the surrounding connective tissue was much less in the ErL treatment than that in the ElS, which suggests that the ErL can be used more safely for periodontal treatment. Furthermore, the minimal thermal influence to the dental pulp following ErL treatment might explain the less painful treatment by ErL during the intra- and postoperative periods [34]. Also, although Hsp72/73 and Hsp47 expressions were observed remote from the treated surface in the ElS sites, postoperative tissue degradation did not extend to the border of these expressions, which suggests that some parts, close to the expression sites, in the non-immunoreactive area, remained without collagen denaturation and worked as a structural scaffold for cell migration during wound healing [33].

The difference in progress of wound healing between the ErL and ElS was clarified by Hsp47 expression. As wound healing progressed, Hsp47 expression moved from the intact connective tissue area to the wound area. This phenomenon

was observed earlier in the ErL than in the ElS. Since the higher expression of Hsp47 indicates ongoing wound healing, the above immunohistochemical finding demonstrates faster healing in the ErL sites than that of the ElS. PCNA is a cell cycle-related nuclear protein, and the cell labeling is directly correlated with the proliferative state of the cell [35–37]. Thus, PCNA expression in the epithelial basal cell layer indicates the progress of re-epithelialization [38, 39]. After surgery, PCNA expression was detected in the epithelial tissue including the basal cell layer in both treatments, and the expression disappeared earlier in the ErL sites than in the ElS. This finding is in accordance with the result of the histometric analysis demonstrating early completion of re-epithelialization in the ErL.

Taken together, the present study demonstrated that the ErL ablation of gingival tissue caused minimal damage to surrounding tissue and exhibited faster and favorable gingival tissue healing compared to the ElS. These results suggest that ErL irradiation has therapeutic benefits for patients and operators and can be considered a safe and suitable tool for periodontal soft tissue management.

Acknowledgments This study was supported in part by a grant from the Global Center of Excellence (GCOE) Program for International Research Center for Molecular Science in Tooth and Bone Diseases at Tokyo Medical and Dental University from the Ministry of Education, Culture, Sports, Science and Technology of Japan, and by a Grant-in-Aid for Scientific Research (C) (22592308) to A.A. from the Japan Society for the Promotion of Science.

References

1. Aoki A, Sasaki KM, Watanabe H, Ishikawa I (2004) Lasers in nonsurgical periodontal therapy. Periodontol 2000 36:59–97
2. Ishikawa I, Aoki A, Takasaki AA (2004) Potential applications of erbium:YAG laser in periodontics. J Periodontal Res 39:275–285
3. Cobb CM (2006) Lasers in periodontics: a review of the literature. J Periodontol 2000 77:545–564
4. Ishikawa I, Aoki A, Takasaki AA, Mizutani K, Sasaki KM, Izumi Y (2009) Application of lasers in periodontics: true innovation or myth? Periodontol 50:90–126
5. Pang PAS, Aoki A, Coluzzi D, Obeidi A, Olivi G, Parker S, Rechmann P, Sulewski J, Sweeney C, Swick M, Yung F (2011) Laser energy in oral soft tissue applications. J Laser Dent 18:123–131
6. Izumi Y, Aoki A, Yamada Y, Kobayashi H, Iwata T, Akizuki T, Suda T, Nakamura S, Wara-Aswapati N, Ueda M, Ishikawa I (2011) Current and future periodontal tissue engineering. Periodontol 2000 56:166–187
7. Hale GM, Querry MR (1973) Optical constants of water in the 200-nm to 200-μm wavelength region. Appl Opt 12:555–563
8. Walsh JT Jr, Flotte TJ, Deutsch TF (1989) Er:YAG laser ablation of tissue: effect of pulse duration and tissue type on thermal damage. Lasers Surg Med 9:314–326
9. Schwarz F, Sculean A, Georg T, Reich E (2001) Periodontal treatment with an Er: YAG laser compared to scaling and root planing. A controlled clinical study. J Periodontol 72(3):361–367
10. Gaspirc B, Skaleric U (2007) Clinical evaluation of periodontal surgical treatment with an Er:YAG laser: 5-year results. J Periodontol 78(10):1864–1871
11. Watanabe H, Ishikawa I, Suzuki M, Hasegawa K (1996) Clinical assessments of the erbium:YAG laser for soft tissue surgery and scaling. J Clin Laser Med Surg 14:67–75
12. Aoki A, Watanabe H, Namiki N, Takiguchi T, Miyazawa Y, Suzuki M, Hasegawa K, Ishikawa I (2003) Periodontal soft tissue management with a high pulse rate Er:YAG laser. Int Congr Ser 1248:367–369
13. Aoki A, Ishikawa I (2004) Application of the Er:YAG laser for esthetic management of periodontal soft tissues. Proceedings of the 9th international congress of laser in dentistry, pp 21–24
14. Rosa DS, Aranha AC, Eduardo Cde P, Aoki A (2007) Esthetic treatment of gingival melanin hyperpigmentation with Er:YAG laser: short-term clinical observations and patient follow-up. J Periodontol 78:2018–2025
15. McGuire MK, Scheyer ET (2011) Laser-assisted flapless crown lengthening: a case series. Int J Periodontics Restorative Dent 31: 357–364
16. Takei HH, Carranza FA (2006) Gingival surgical techniques. In: Newman MG, Takei HH, Klokkevold PR, Carranza FA (eds) Carranza's Clinical periodontology, 10th edn. Elsevier, St. Louis, p 915
17. Bashetty K, Nadig G, Kapoor S (2009) Electrosurgery in aesthetic and restorative dentistry: a literature review and case reports. J Conserv Dent 12:139–144
18. Ravishankar PL, Satheesh M (2011) Electro surgery: a review on its application and biocompatibility on periodontium. Indian J Dent Advancements 3(2):492–498
19. Glickman I, Imber LR (1970) Comparison of gingival resection with electrosurgery and periodontal knives—a biometric and histologic study. J Periodontol 41:142–148
20. Simon BI, Schuback P, Deasy MJ, Kelner RM (1976) The destructive potential of electrosurgery on the periodontium. J Periodontol 47:342–347
21. Wilhelmsen NR, Ramfjord SP, Blankenship JR (1976) Effects of electrosurgery on the gingival attachment in rhesus monkeys. J Periodontol 47:160–170
22. Leach J, Manning S, Schaefer S (1993) Comparison of two methods of tonsillectomy. Laryngoscope 103:619–622
23. Craig EA (1985) The heat shock response. CRC Crit Rev Biochem 18:239–280
24. Lindquist S (1986) The heat-shock response. Annu Rev Biochem 55: 1151–1191
25. Kregel KC (2002) Heat shock proteins: modifying factors in physiological stress responses and acquired thermotolerance. J Appl Physiol 92:2177–2186
26. Silver JT, Noble EG (2012) Regulation of survival gene hsp70. Cell Stress Chaperones 17:1–9
27. Satoh M, Hirayoshi K, Yokota S, Hosokawa N, Nagata K (1996) Intracellular interaction of collagen-specific stress protein HSP47 with newly synthesized procollagen. J Cell Biol 133: 469–483
28. Nagai N, Hosokawa M, Itohara S, Adachi E, Matsushita T, Hosokawa N, Nagata K (2000) Embryonic lethality of molecular chaperone hsp47 knockout mice is associated with defects in collagen biosynthesis. J Cell Biol 150:1499–1506
29. Welch WJ (1992) Mammalian stress response: cell physiology, structure/function of stress proteins, and implications for medicine and disease. Physiol Rev 72:1063–1081
30. Li GC, Li LG, Liu YK, Mak JY, Chen LL, Lee WM (1991) Thermal response of rat fibroblasts stably transfected with the human 70-kDa heat shock protein-encoding gene. Proc Natl Acad Sci USA 88: 1681–1685
31. Ruell PA, Hoffman KM, Chow CM, Thompson MW (2004) Effect of temperature and duration of hyperthermia on HSP72 induction in rat tissues. Mol Cell Biochem 267:187–194

32. Nagata K, Yamada KM (1986) Phosphorylation and transformation sensitivity of a major collagen-binding protein of fibroblasts. J Biol Chem 261:7531–7536
33. Yamasaki A, Tamamura K, Sakurai Y, Okuyama N, Yusa J, Ito H (2008) Remodeling of the rat gingiva induced by CO_2 laser coagulation mode. Lasers Surg Med 40:695–703
34. Zeredo JL, Sasaki KM, Yozgatian JH, Okada Y, Toda K (2005) Comparison of jaw-opening reflexes evoked by Er:YAG laser versus scalpel incisions in rats. Oral Surg Oral Med Oral Pathol Oral Radiol Endod 100:31–35
35. Celis JE, Celis A (1985) Cell cycle-dependent variations in the distribution of the nuclear protein cyclin proliferating cell nuclear antigen in cultured cells: subdivision of S phase. Proc Natl Acad Sci USA 82:3262–3266
36. Kurki P, Vanderlaan M, Dolbeare F, Gray J, Tan EM (1986) Expression of proliferating cell nuclear antigen (PCNA)/cyclin during the cell cycle. Exp Cell Res 166:209–219
37. Kurki P, Ogata K, Tan EM (1988) Monoclonal antibodies to proliferating cell nuclear antigen (PCNA)/cyclin as probes for proliferating cells by immunofluorescence microscopy and flow cytometry. J Immunol Methods 109:49–59
38. Mittal KR, Demopoulos RI, Goswami S (1993) Proliferating cell nuclear antigen (cyclin) expression in normal and abnormal cervical squamous epithelia. Am J Surg Pathol 17:117–122
39. Warnakulasuriya KA, Johnson NW (1993) Comparison of isotopic and immunohistochemical methods of studying epithelial cell proliferation in hamster tongue. Cell Prolif 26: 545–555